PAPER

Multifunctional phononic meta-material actuated by the phase transition in water

To cite this article: Yuqi Jin et al 2023 Phys. Scr. 98 065008

View the <u>article online</u> for updates and enhancements.

You may also like

- <u>CEWQO Topical Issue</u> Mirjana Bozic and Margarita Man'ko
- Metamaterial-plasma based hyperbolic material for sensor, detector and switching application at microwave region
 Asish Kumar, Narendra Kumar, Girijesh N Pandey et al.
- A Low-Cost Aptamer Immobilization
 Technique for the Selective Detection of
 Protein Biomarkers Using Electrochemical
 Impedance Spectroscopy
 Niazul Islam Khan and Edward Song

Physica Scripta



RECEIVED 6 March 2023

REVISED 17 April 2023

ACCEPTED FOR PUBLICATION 26 April 2023

PUBLISHED 4 May 2023

PAPER

Multifunctional phononic meta-material actuated by the phase transition in water

Yuqi Jin¹, Teng Yang², Narendra B Dahotre² and Arup Neogi^{1,3,*}

- Department of Physics, University of North Texas, Denton, TX 76203, United States of America
- ² Department of Materials Science and Engineering, University of North Texas, Denton, TX 76207, United States of America
- Institute of Fundamental and Frontier Sciences, University of Electronic Science and Technology of China, Chengdu, 611731, People's Republic of China
- Author to whom any correspondence should be addressed.

E-mail: arupn@yahoo.com

Keywords: acoustic filter, acoustic splitter, acoustic lensing, acoustic transparency, phase transformation

Abstract

The functionality of thermally active phononic crystals (PnC) and metamaterials can be greatly enhanced by utilizing the temperature-dependent physical characteristics of heat-sensitive materials within the periodic structure. The phase transformation between water and ice occurs within a narrow range of temperatures that can lead to significant changes in its acoustic transmission due to the modification of the elastic properties of periodic phononic structures in an aqueous medium. A phononic crystal with acrylic scatterers in water is designed to function as an acoustic filter, beam splitter, or lensing based on the device's temperature due to changes in the phase of the ambient medium. The transition from room temperature to freezing point reduces the contrast in acoustic properties between the ice-lattice and the scatterer materials (acrylic) and switches off the metamaterial of the water-based PnC. The numerically simulated equi-frequency contours and wave propagation characteristics demonstrate the switchable meta-material to the periodic phononic structure's normal behavior due to the phase transition of water. Effects such as Van Hove's singularity and filamentation-like effects in an acoustic meta-material system can be thermally tuned.

1. Introduction

Phononic crystals (PnC) are artificially engineered periodic structures that can be designed with two materials, ideally with a significant contrast in the elastic or acoustic properties between the scatterer and the ambient background supporting the lattice structure [1]. At long operational wavelengths, these two- or three-dimensional periodic lattice structures can behave as an effective medium within the homogenization approximation [2, 3]. At higher frequencies, with the wavelength approaching the periodicity of the PnC, the anomalous or nonlinear dispersion in the transmission frequency ranges leads to the presence of exotic physical characteristics, such as negative index of refractions [4] that can lead to unguided wave modes or anomalous reflections [5], and has been categorized into acoustic metamaterial. Like semiconductors in electronics, phononic crystals, as 'acoustic semiconductors', are designed and studied to modify and control the propagation of waves at the acoustic, elastic, or vibrational frequencies [6]. Recent trends in this field have resulted in several smart and functional phononic structures such as filters [7], splitters [8], collimators [9], lenses [10], etc. Such arrangements can be designed in 1D [11], 2D [12], and even 3D [13] configurations. Appropriate scaling of these phononic crystals can effectively yield applications over a wide range of frequencies ranging from mechanical vibrations [14], sound [12], and even thermal dissipation [15]. These structures can be designed with special and unique properties, including self-collimations [16], cloaking [17], and pulse decomposition [18].

In addition to designing tunable acoustic PnCs at various operating frequencies, there has been renewed interest in using these periodic structures with metamaterial behavior to control the propagation of acoustic waves that defies the conventional laws of wave propagation. Compared to semiconductors or photonic crystals,

the relatively large size of phononic crystals makes it easier to use external fields such as light [19], magnetic fields [20], mechanical motions [12], and thermal transport [10] to control the propagation of acoustic waves. Optical and magnetically tunable PnCs can be fast and precise among these external actuation mechanisms of controlling phononic crystals. However, the size of the phononic crystal structures is a limitation due to the poor penetration of the electromagnetic wave in common solid and liquid materials. Mechanically tunable PnCs primarily achieved by rotating the asymmetric scatterers [12] are challenging to scale down to operate at higher frequencies due to the bulky mechanical components. On the contrary, although thermal tunability responds slowly, there are no clear size limitations on the applied structures, and it has been considered an efficient mechanism for designing tunable PnCs. Temperature-tunable PnCs have been reported [19] using thermalresponsive hybrid hydrogel. In order to achieve strong physical properties contrast in the two distinguishable states, phase transformation is a convenient and effective mechanism [21]. Around room temperature, thermal responsive hydrogels [22] or liquid metal Gallium [23] has been applied to enhance the stark contrast in the physical properties of the materials composing the periodic structure. However, due to the strong volumetric change during the phase transformation in hydrogels, the contact between the hydrogels and other metals/ plastics are generally poor. Liquid Gallium also does not bind well with polymers or ceramics. It also induces embrittlement on other metals [24] and is shapeless in liquids, which increases the challenge of designing tunable PnC with material homogeneity. Water despite its high specific heat is an ideal environment for supporting phononic crystals with metallic or polymeric scatterers. Furthermore, the tunability in PnC lattice material due to the transformation from water to ice due to a change in temperature has yet to be explored. Due to the significant changes in water from room temperature to freezing point occurring within a narrow temperature range, a strong contrast in the physical properties can be achieved due to the phase transition from the amorphous form to crystalline states of the supporting ambient medium supporting the phononic crystal.

In the present work, we designed the thermal tunable PnC based on an acrylic-based phononic crystal in a water medium. PnC in water as an ambient material is a commonly existing system [25], especially in ultrasound range operating frequencies. A drop in the room temperature by 20 °C can result in the formation of ice at the freezing point with a significantly higher speed of sound value c along with a slight reduction in density ρ . As a result, the product $K = \rho c^2$, shows a clear increase in the elastic modulus K due to the phase transformation from water to ice, leading to a vastly different vibrational response. To further accentuate the contribution of the change in background medium from water to ice, acrylic is considered the scatterer material as it has clear physical contrast with liquid water but is mechanically comparable to ice in the solid phase [26]. The tunability between a high-contrast water-acrylic PnC and a relatively low-contrast ice-acrylic PnC can yield efficient switching behavior of acoustic bandgaps, acoustic splitting, and acoustic collimation.

2. Methods

The band structure and equi-frequency (also called iso-frequency) contours were numerically calculated by the plane wave expansion method in the range between -0.5 and 0.5 with step interval 0.01 for both k_x and k_y . Numerical simulations of acoustic wave propagation behaviors were conducted using COMSOL Multiphysics software 5.5. Liquid water properties were obtained from the COMSOL material library with a speed of sound c=1478 m s⁻¹ at 20 °C ambient temperature, and the density of 998 kg m⁻³. The speed of sound values and density of acrylic were set to 2718 m s⁻¹ (longitudinal), 1370 m s⁻¹ (transversal), and 1170 kg m⁻³, respectively, based on the literature survey [27, 28]. The acoustic properties of ice were obtained from the references [26]. The PnCs are considered with dimensions 10×10 , 20×25 , and 12×15 for the tunable filter, tunable splitter, and tunable lens, respectively. The studied frequency range was 150 kHz to 650 kHz, 595 kHz, and 680 kHz for the tunable filter case, tunable splitter case, and tunable lens, respectively. The acoustic source has emission amplitude at 1 μ Pa, where the 0 dB reference line was also 1 μ Pa. In the simulation models, the ambient water areas were considered with impedance-matched boundary conditions to eliminate internal reflections reflection from the outer boundaries.

3. Results and discussion

In this work, we select the conventional PnC design of a fully symmetric scatterer in a homogenous background medium of water or ice for demonstrations. Water or ice is the ambient medium for the phononic crystal in a square lattice configuration with a periodicity of a=2.5 mm. The scatterers were presumed to be composed of cylindrically shaped acrylic with rods with a diameter $\phi=1.5$ mm and appear as a circular geometry under 2D view. The filling fraction is about 50%. The tunability is realized from the difference in the operating condition at room temperature (20 °C) to that at the freezing point (0 °C). The speed of sound values in liquid water and solid-phase ice are obtained from the literature and summarized in figure 1(A) [26]. The existence of air bubbles

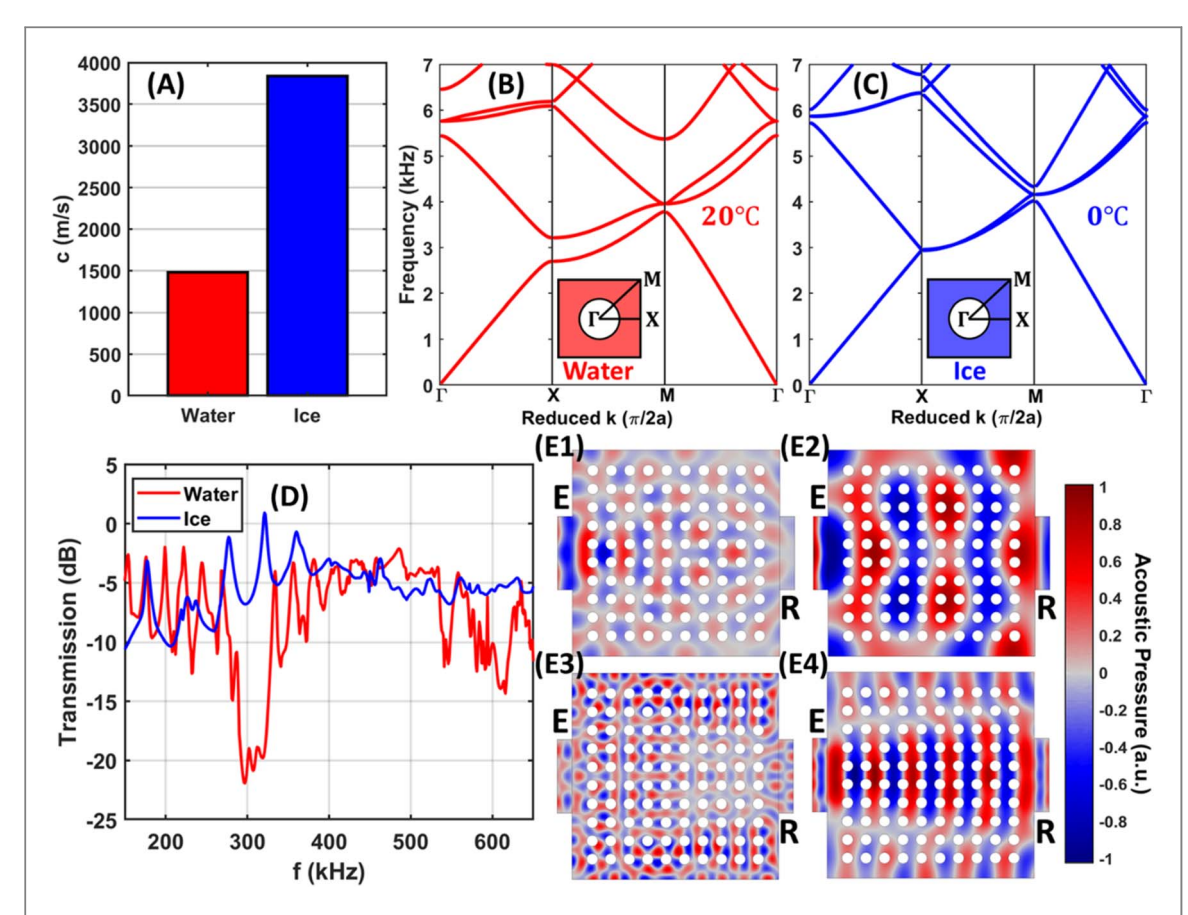


Figure 1. Thermal tunable band structure and acoustic filtering. (A) Speed of sound comparison between water and ice based on the literature [26]. (B) and (C) along ΓX , XM, and ΓM directions from frequency range 0 to 700 kHz for water/acrylic PnC and ice/acrylic PnC. (D) Comparison of transmission spectrums from 10×10 PnCs with water lattice and ice lattice. (E) Acoustic pressure maps on the 10×10 PnCs at 310 kHz in water PnC (E1), 310 kHz in ice PnC (E2), 610 kHz in water PnC (E3), and 610 kHz in ice PnC (E4). E and R refer to emission source and receiver.

can reduce the speed of sound in both water and ice. Thereby, we consider an ideal air-free condition in both states of matter. As the bar diagram illustrates, the phase transition from amorphous to crystalline state enhances the velocity of sound in ice compared to that in water. It offers significantly different physical properties due to a 20 °C difference. From the plane wave expansion approximations, the analytical band structures in the first Brillouin zone of water/Acrylic and ice/Acrylic PnCs are shown in figures 1(B) and (C), along Γ X (parallel), XM(perpendicular), and Γ M (45 ° diagonal) directions under the Bloch vectors in the unit $\pi/2a$. With an identical size and periodicity of the square lattice, the water-to-ice transformation induces a significant variation in the band structures. In the water-based PnC (figure 1(B)), the 1st semi-bandgap occurs around 300 kHz along Γ X. In ice-based PnC (figure/1C), we observe the absence of the 1st bandgap around 300 kHz due to the much weaker physical properties contrast between background ice and the acrylic scatterers compared to the strong difference between water and acrylic. The width of the 2nd and 3rd semi-band gaps around 550 kHz and 600 kHz in water PnC are also significantly reduced in the ice-based PnC.

The transmission spectrums are numerically simulated for a 10×10 PnC by assigning the background material as water or ice (figure 1(D)). In figures 1E1 and 1E2, the acoustic wave propagation behaviors at 310 kHz are illustrated in terms of acoustic pressure distributions. As stated earlier, the absence of the bandgaps can also be observed by comparing the two frequency spectra. As water has a much slower velocity of sound, in figure 1(E1), the wavelength is expectedly shorter than in the ice-based PnC, as shown in figure 1(E2). With just ten periods of the PnC, a fully forbidden transmission of the ultrasonic wave in water PnC (figure 1(E1)) can be fully transparent in the ice-based PnC (figure 1(E1)). Similar behaviors can also be obtained in the 2nd bandgap around 610 kHz of the water-based PnC (figure 1(E3) to figures 2(E4), ice PnC). As PnCs are commonly claimed to be acoustic wave filters, a change in temperature of the water around the phononic crystal from room temperature to the freezing point can yield a 15 dB change in the transmissivity of the signal within ten periods. In addition, at about 312 kHz, a clear resonance mode (peak above 0 dB reference line) can be found on the ice-based PnC, where the water PnC yields a transmission gap at that frequency. With a longer length of the PnC due to enhanced periodicity, the transmission difference at 312 kHz is expected to be even stronger compared with negligible energy loss on resonance (ice-based PnC) and exponential decay in gap frequency (water-based PnC).

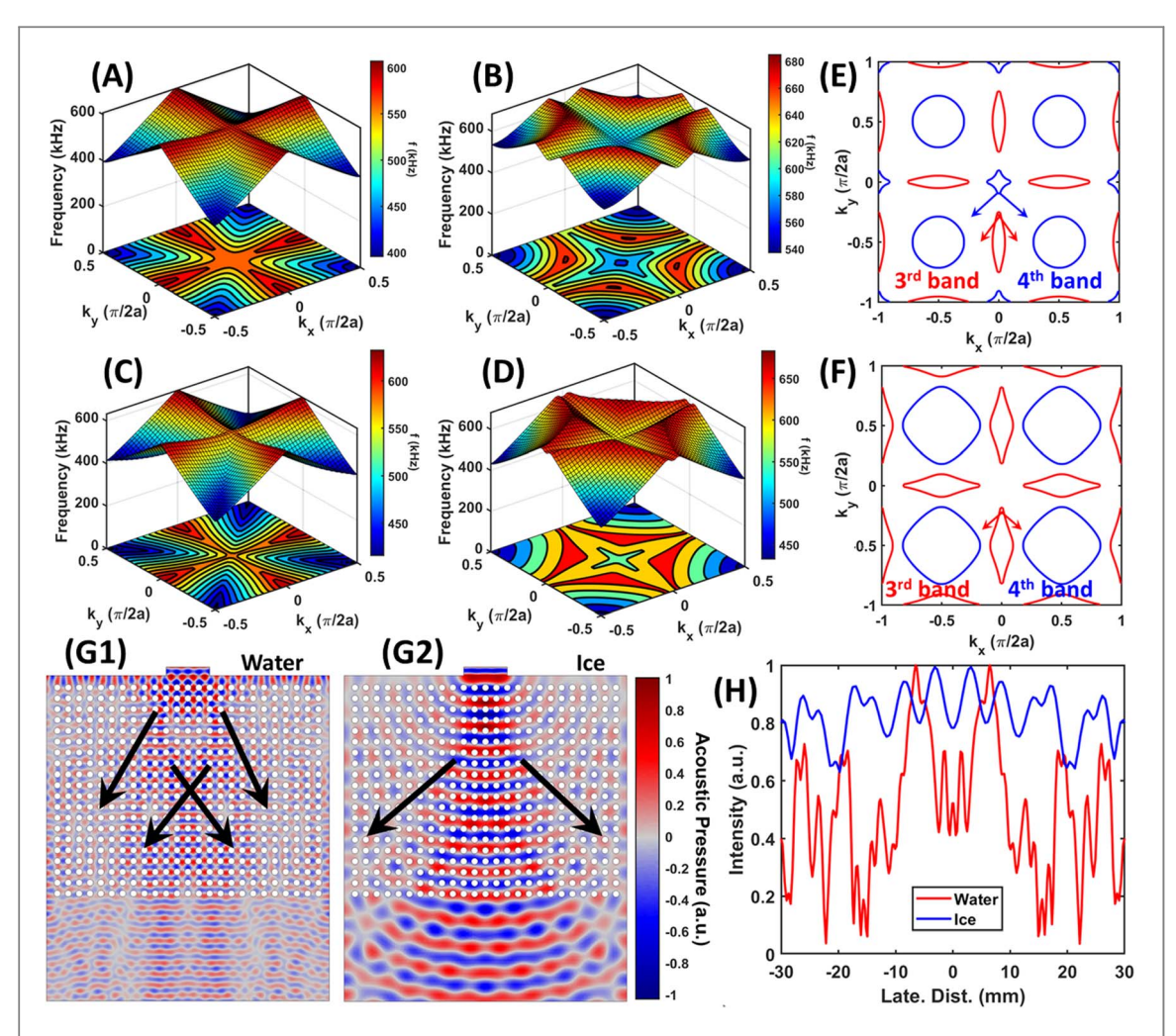


Figure 2. Thermal tunable acoustic splitter. (A), (B), (C), and (D) are the EFCs of the third transmission band of water PnC, the fourth transmission band of water PnC, the EFCs of the third transmission band of ice PnC, and the fourth transmission band of ice PnC, respectively (E) and (F) Combined EFCs in the third and fourth transmission bands corresponding to frequency 595 kHz of the water PnC and ice PnC, respectively. (G1) and (G2) are the acoustic pressure maps at 595 kHz of the water PnC case and ice PnC case, respectively. (H) Lateral cut lines from (G1) and (G2) in terms of acoustic intensity at the outcoming ambient regions.

Secondly, in the band diagram (figures 1(B) and (C)), we observe two additional bands (3rd and 4th) on the Γ X around 595 kHz in the PnC underwater. However, only one transmission band is retained in the ice-based PnC case. The difference in the number of bands indicates that two vibrational modes can be simultaneously excited with one monochromatic source with the normal incidence in the water-based PnC around 595 kHz. However, only one responsive mode can be excited in the ice-based PnC at the same operating frequency with an identical source. To fully analyze this behavior, we further calculate the dispersion relation in a 2D Bloch vector domain with all the possible angles to obtain the equi-frequency contours (EFCs). The EFCs (figures 2(A)–(D)), $\omega(k_x, k_y)$, carry the additional dimension information in terms of energy, translated into frequency. Each 3D surface represents a single transmission band along all the wave vector directions. The 2D surface contours are the projections of the 3D EFCs. From the observations, all the 3rd/4th bands of water-based PnC (figures 2(A) and (B)) and the 3rd/4th bands of ice-based PnC (figures 2(C) and (D)) cover the frequency range included around 595 kHz, and highly geometrically comparable. Thus, we plot the summary contours with both transmission bands separately for water-based PnC (figure 2(E)) and ice-base dPnC (figure 2(E)) using a single contour line at 595 kHz from each transmission band.

In the summarized EFCs at 595 kHz (figures 2(E) and (F)), we observe the topological offset of the contour lines for half of the first Brillouin zone between the 3rd and 4th bands, similar to Van Hove's singularity-based effect. For a normal incidence, we define the source vector k_i propagating along the k_y axis direction from the positive to negative (center to down). Following the Bragg law $k_i = G + k_r$, the resulting refracted vectors k_r occurs when the incidence meets the contour line (reciprocal lattice vector G). We note that the refraction k_r in this case, refers to the refracted vectors within the PnC and not the outcoming refraction. The directions of the refracted vectors are perpendicular to the curvature of the contour lines pointing to a path where the frequency gradient is greater than 1. With a finite-size plane wave source with normal incidence, not all the wave vectors

travel in parallel with normal direction due to the near field effect. Hence, in the summarized EFCs, we consider the source wave vector content to have a slight orientational deviation from the perfect vertical direction. On the central vertical lines, we can observe the normal incidence source wave at 595 kHz can excite both the 3rd and 4th bands, as quasimomentum-matching conditions, in water PnC refracted to the different directions with different modes (figure 2(E)). On the contrary, in figure 2(F), although both transmission bands are presented in the summary contour, the 4th transmission band does not equip any available mode around the normal incidence direction. Only the 3rd band of the ice crystal offers one excitation mode that is excited at the normal incidence. We note again here that the refraction arrows in figures 2(E) and (F) refer to the refracted illustrations of wave vector directions within the PnCs, but not the transmitted refractions outside the PnCs. In the existing literature, beam splitting effects were realized in both photonic crystals and phononic crystals with various mechanism including anisotropic zero effective density and hyperbolic dispersion relations [29, 30] which induced the beam splitting effects directly in the metamaterial structure. On the contrary, the method proposed in this work uses multi-mode interference to form splitting acoustic beam in the outcoming medium instead of inside the phononic structure. The mechanism is simpler with respect to literature proposed methods but occurs limitations such as source beam sensitive and PnC length sensitive.

The numerical simulations also enable a bulk view of the wave propagation characteristics through the water-based PnC (figure 2(G1)) and the ice-based PnC (figure 2(G2)) using a model with 20 periods along the wave propagation direction at 595 kHz. In the case of water-based PnC (figure 2(G1)), an anisotropic interference is observed due to the contribution from multiple modes of refractions within the PnC. As a result, the wave transmitted from the phononic crystal at the output exhibits a beam-splitting-like effect due to the interference. On the contrary, in figure 2(G2), the refractions in ice-based PnC are more isotropic and dispersed due to the absence of any interference with the additional mode. At the outgoing region where the transmitted wave exits the PnCs, a horizontal outline is selected for obtaining the lateral sound intensity profiles (figure 2(H)) for both water-based PnC and ice-based PnC (figures 2(G1) and (G2)). As a result of the multi-mode interference, the water-based PnC case shows a distinctive splitting effect from the source beam to 2 transmitted beams (red line). Due to a 20 °C reduction in temperature toward the freezing point, the ice-based PnC can merge the two components of the split beams into a single isotropic mode that simply spreads along the propagation direction due to linear dispersion (blue line).

The acoustic lensing effect in metamaterials is also a broadly studied topic in phononic crystals. Due to the proposed thermal tunability of the PnC, lensing or collimation effects can also be achieved. With proper transmission band selection, a thermally switchable lensing effect can be realized by making transitions between water-based PnC and ice-based PnC. In the band structures (figures 1(B) and (C)), we selected the 5th transmission band to study in this work. On the ice PnC (figure 1(C)), we observe an approximately linear 5th band curve which is highly parallel to the 1st transmission band in the ΓX direction. However, on the water PnC (figure 1(B)), the 5th transmission band is clearly nonlinear with changing slope. On the EFCs (figures 3(A) and (B)), the water PnC (figure 3(A)) shows a consistent flat-edge contour in the low-frequency range (under 700 kHz), indicating a strong self-collimation effect on the wave with around normal incidence under 700 kHz. The self-collimation effect, or filamentation-liked behavior, is caused by the rapidly changing index of refraction (flat edge) on the EFC curvature (figure 3(C)). It implies that the direction of the refracted wave is relatively independent of the incident angle, as the central square and the black arrows are illustrated in figure 3(C). However, the ice PnC (figure 3(B)) presents a circular-to-square transition from 650 kHz to 700 kHz. The circular EFC refers to a uniform material-like behavior where the index of refraction is not incident angle dependent. Hence, simple and consistent spreading-liked behavior is expected based on the circular EFC in ice PnC, as shown in figure 3(D). To visualize the thermal tunable lensing effects due to the different topologies in EFCs, we conduct two numerical simulations using the model demonstrated in figure 3(E).

We proposed 3D PnC cases using axial symmetric models to construct ring-array-like lenses in the numerical simulations. Both the water-based PnC lens (figure 3(F)) and ice-based PnC lens (figure 3(H)) have identical geometrical dimensions. As stated in the methods section, the transducer and outside ambient are considered to be liquid water in the lens modeling. The difference between the two simulation models is the medium (water and ice) within the region of the acrylic scattering rods. As figure 3(E) illustrates, the acoustic source transducer has a size of about 0.4 of the width of the PnC lenses. In the water-based-PnC lens, the self-collimation effect occurs as the flat-edge EFC shown in figure 3(C). In contrast, the normal spreading refractions occur in the ice-based PnC lens as the circular EFC indicated, respectively. Due to the self-collimation or filamentation of the parallel propagating wave vector arrangement on the water PnC lens, the original self-focusing near field effect from the transducer filaments into multiple beams with focusing arrays formed from different spatial lateral positions on the outcoming edge of the water PnC lens (the edge farther from and parallel to the transducer). This effect is similar to the self-phase modulation effect observed in nonlinear optics for self-focused beams in a medium with high third-order nonlinearity. The multiple-focusing array concentrates the acoustic energy in a relatively narrow spatial region along the wave propagation direction, which forms a narrow

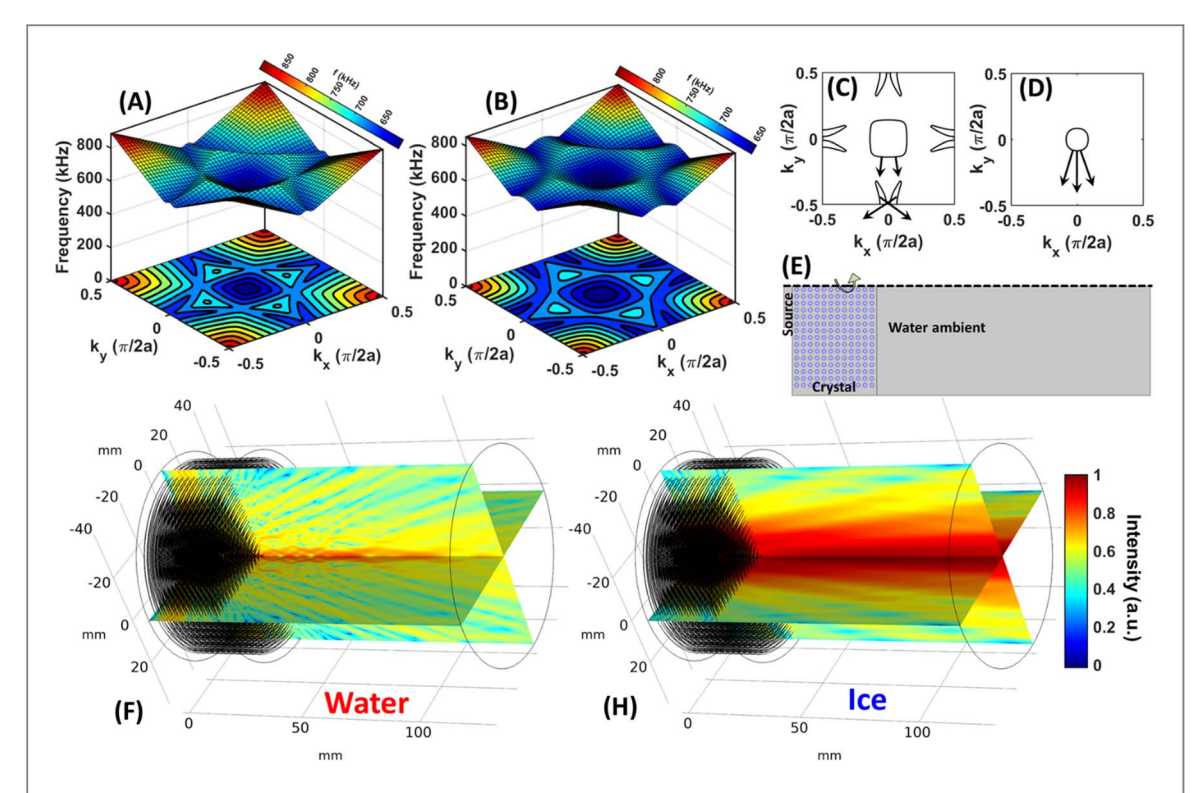


Figure 3. Thermal tunable acoustic lens. (A) and (B) are the EFCs of the fifth transmission band of water PnC and ice PnC. (C) and (D) Selected EFCs in the fifth transmission bands corresponding to frequency $680\,\mathrm{kHz}$ of the water PnC and ice PnC. (E) Configuration of the numerical simulation models for estimating the tunable lensing effect. (F) and (H) are the acoustic intensity distributions at $680\,\mathrm{kHz}$ of the water PnC case and ice PnC case, respectively.

lateral width collimation beam in figure 3(F). Due to the cooling-induced transition from a water-based PnC lens to an ice-based PnC lens, the narrow collimating lensing effect can be cut-off and tuned to a uniform material-like spreading behavior with an approximate incidence angle-independent index of refraction.

This study demonstrated freezing point and room temperature as two major states for obtaining strong acoustic property transition by the water/ice phase transition. However, the proposed design is not limited to such two temperature points. Within the liquid state, the water still has clear temperature-dependent acoustic property variation. Although the temperature-dependent property variation within liquid state is not as strong as shifting to solid state, finer temperature-dependent acoustic property tunability can be potentially feasible to achieve within the liquid state. Finer thermal tunable filtering frequency range and finer thermal tunable focal distance can be realized in water/acrylic PnC based filter and lens respectively.

For practical case, a box-liked container can be fabricated with the acrylic rods array (scatterers) inside. The infilled water is a lattice material which can be tuned into ice by changing the temperature. The device fabrication is obvious. However, in detail, it is challenged to perform practical experiments without thorough experimental designs. Especially for the ice/acrylic PnC case, the bonding between such two solid materials might not be strong enough. Hence, the ice/acrylic phononic crystal needs to be placed in water ambient (coupling) for transmission experiments. The ambient water can serve as a coupler and fill the gap between ice and acrylic. To control the transitions between the water and ice states, the entire PnC needs to be closed clamber liked device to prevent unnecessary mass conversion. For example, an acrylic box mentioned can be a potential candidate. To vary the temperature of the device, thermoelectrical device (TED) can be good tool to perform cooling or heating processing.

With the design proposed in the study, heating and cooling processes are considered as the suitable approach to shift the states of the PnC. In thermodynamics, cooling is not the only method to perform water to ice transition. The alternative approach can be pressurization. However, applying strong pressure to the PnC system can potentially introduce cracks on the acrylic scatterers. With metal scatterers, pressurization might be able to serve as an alternative approach in extreme conditions. However, it is not a suitable method to propose in the work. With the proposed system, fluid motion or local vortex might be able to enrich the control freedom under the water/acrylic PnC state. The additional Doppler effect can potentially introduce nonreciprocity or anisotropy transmission in the system which can be one of the directions for future studies.

The proposed method to achieve strong temperature tunability in PnC can be applied to other phononic periodical systems, such as superlattice, as long as the background medium (lattice material) is homogenous and

temperature tunable. For the geometry of the scatterers, some technical issues need to be considered associated to complex geometrical scatterers such as the wetted angles between the liquid lattice and solid scatterers. In the case that the lattice material can have comparable contacting area with the scatterers in both liquid and solid, the proposed design can be alternatively applied to the systems leading to the similar temperature-dependent switching functionality. In the acoustical physics field, phononic crystal is considered as a potential approach to perform acoustic filtering, noise reduction or beamforming technique. The practical applications of functional PnC or acoustic metamaterials are currently not broad enough. Most of the studies are still under laboratory conditions. The proposed design has a strong impedance mismatch with air. Hence, the potential occasions of the design should be underwater applications instead of the applications in air ambient. The potential applications could be underwater acoustic filtering and underwater acoustic noise reduction device with the thermal controllable switch. Furthermore, the tunable lensing application would also be interesting to explore. As known, the ice/acrylic PnC lens behaves similar to a natural material, whereas the water/acrylic PnC lens behaves as an acoustic metamaterial. Hence, the thermal focusing to collimation tunability can be realized with on-off switching.

4. Conclusion

In conclusion, we designed and analyzed a temperature-tunable phononic metamaterial with water lattice and acrylic scatterers in this work. Strong acoustic propagation behavior modifications are predicted due to the phase transformation of water to ice achieved by lowering the temperature to the freezing point. By numerical simulation, the presence of transmission bandgaps, additional transmission bands, and the flat edge of the equifrequency curve can be switched off by tuning the water-ambient lattice to an ice-ambient lattice. Without adjusting the operating frequency, the temperature-tunable phononic metamaterial breaks the limit of conventional designs and offers flexible functionality. The numerical demonstrations on those tunable behaviors were conducted to perform as temperature switchable acoustic filters, splitter, and collimation lens.

Data availability statement

The data cannot be made publicly available upon publication because they are not available in a format that is sufficiently accessible or reusable by other researchers. The data that support the findings of this study are available upon reasonable request from the authors.

Funding and acknowledgments

This work is supported by an EFRI Grant No. 1741677 from the National Science Foundation.

Conflict of interest

The authors have no competing interests.

ORCID iDs

References

- [1] Kushwaha M S, Halevi P, Dobrzynski L and Djafari-Rouhani B 1993 Acoustic band structure of periodic elastic composites *Phys. Rev. Lett.* 71 2022
- $[2] \ Hou\ Z, Wu\ F, Fu\ X\ and\ Liu\ Y\ 2005\ Effective\ elastic\ parameters\ of\ the\ two-dimensional\ phononic\ crystal\ Phys.\ Rev.\ E\ 71\ 037604$
- [3] Śmigaj W and Gralak B 2008 Validity of the effective-medium approximation of photonic crystals Phys. Rev. B 77 235445
- [4] Bucay J et al 2009 Positive, negative, zero refraction, and beam splitting in a solid/air phononic crystal: theoretical and experimental study Phys. Rev. B 79 214305
- [5] Jin Y, Walker E, Choi T-Y, Neogi A and Krokhin A 2022 Simultaneous negative reflection and refraction and reverse-incident right-angle collimation of sound in a solid-fluid phononic crystal the Journal of the Acoustical Society of America 151 2723
- [6] Dowling J P 1992 Sonic band structure in fluids with periodic density variations J. Acoust. Soc. Am. 91 2539–43

[7] Qiu C, Liu Z, Mei J and Shi J 2005 Mode-selecting acoustic filter by using resonant tunneling of two-dimensional double phononic crystals Appl. Phys. Lett. 87 104101

- [8] Li J, Wu F, Zhong H, Yao Y and Zhang X 2015 Acoustic beam splitting in two-dimensional phononic crystals using self-collimation effect J. Appl. Phys. 118 144903
- [9] Zubov Y et al 2020 Long-range nonspreading propagation of sound beam through periodic layered structure Commun. Phys. 3 1-8
- [10] Walker E L, Reyes-Contreras D, Jin Y and Neogi A 2019 Tunable hybrid phononic crystal lens using thermo-acoustic polymers ACS Omega 4 16585–90
- [11] Croy A, Cain P and Schreiber M 2011 Anderson localization in 1D systems with correlated disorder Eur. Phys. J. B 82 107
- [12] Dhillon J, Bozhko A, Walker E, Neogi A and Krokhin A 2021 Localization of ultrasound in 2D phononic crystal with randomly oriented asymmetric scatterers J. Appl. Phys. 129 134701
- [13] Semeghini G et al 2015 Measurement of the mobility edge for 3D Anderson localization Nat. Phys. 11 554
- [14] Skipetrov S E and Beltukov Y M 2018 Anderson transition for elastic waves in three dimensions Phys. Rev. B 98 064206
- [15] Juntunen T, Vänskä O and Tittonen I 2019 Anderson localization quenches thermal transport in aperiodic superlattices Phys. Rev. Lett. 122 105901
- [16] Jiménez N, Picó R, Sánchez-Morcillo V J, García-Raffi L M and Staliunas K 2015 Nonlinear self-collimated sound beams in sonic crystals Phys. Rev. B 92 054302
- [17] Torrent D and Sánchez-Dehesa J 2008 Acoustic cloaking in two dimensions: a feasible approach New J. Phys. 10 063015
- [18] Jin Y, Zubov Y, Yang T, Choi T-Y, Krokhin A and Neogi A 2021 Spatial decomposition of a broadband pulse caused by strong frequency dispersion of sound in acoustic metamaterial superlattice *Materials* 14 125
- [19] Walker E L, Wang Z and Neogi A 2017 Radio-frequency actuated polymer-based phononic meta-materials for control of ultrasonic waves NPG Asia Mater. 9 e350
- [20] Robillard J-F et al 2009 Tunable magnetoelastic phononic crystals Appl. Phys. Lett. 95 124104
- [21] Jin Y, Yang T, Ju S, Zhang H, Choi T-Y and Neogi A 2020 Thermally tunable dynamic and static elastic properties of hydrogel due to volumetric phase transition *Polymers* 12 1462
- [22] Jin Y, Heo H, Walker E, Krokhin A, Choi T Y and Neogi A 2020 The effects of temperature and frequency dispersion on sound speed in bulk poly (Vinyl Alcohol) poly (N-isopropylacrylamide) hydrogels caused by the phase transition *Ultrasonics* 104 105931
- [23] Yang T, Jin Y, Squires B, Choi T-Y, Dahotre N B and Neogi A 2021 In-situ monitoring and ex situ elasticity mapping of laser induced metal melting pool using ultrasound: numerical and experimental approaches J. Manuf. Processes 71 178
- [24] Rajagopalan M, Bhatia MA, Tschopp MA, Srolovitz DJ and Solanki KN 2014 Atomic-scale analysis of liquid-gallium embrittlement of aluminum grain boundaries *Acta Mater.* 73 312
- [25] Li Z et al 2021 Focus of ultrasonic underwater sound with 3D printed phononic crystal Appl. Phys. Lett. 119 073501
- [26] Vogt C, Laihem K and Wiebusch C 2008 Speed of sound in bubble-free ice J. Acoust. Soc. Am. 124 3613
- [27] Lowery M D, Makker H and Lang A 2002 Effect of the speed of sound in Sensar acrylic lenses on pseudophakic axial length measurements *Journal of Cataract & Refractive Surgery* 28 1269
- [28] Leroy V, Pitura K M, Scanlon M G and Page J H 2010 The complex shear modulus of dough over a wide frequency range J. Non-Newtonian Fluid Mech. 165 475
- [29] Xu C et al 2022 Acoustic beam splitting and cloaking based on a compressibility-near-zero medium Phys. Rev. Appl. 17 054025
- [30] Guo Z, Long Y, Jiang H, Ren J and Chen H 2021 Anomalous unidirectional excitation of high-k hyperbolic modes using all-electric metasources *Advanced Photonics* **3** 036001